ISSN 1070-3284, Russian Journal of Coordination Chemistry, 2014, Vol. 40, No. 1, pp. 16–22. © Pleiades Publishing, Ltd., 2014.
Original Russian Text © I.V. Taidakov, A.N. Lobanov, L.S. Lepnev, A.G. Vitukhnovskii, 2014, published in Koordinatsionnaya Khimiya, 2014, Vol. 40, No. 1, pp. 20–26.

Neodymium(III) Tris(1,3-Bis(1,3-Dimethyl-1*H*-Pyrazol-4-yl)propane-1,3-Dionato)(1,10-Phenanthroline): Synthesis and Photophysical Properties

I. V. Taidakov*, A. N. Lobanov, L. S. Lepnev, and A. G. Vitukhnovskii

Lebedev Physical Institute, Russian Academy of Sciences, Leninskii pr. 53, Moscow, 119991 Russia

**e-mail: taidakov@gmail.com*

Received April 1, 2013

Abstract—The reaction of $NdCl_3$ with 1,3-bis(1,3-dimethyl-1*H*-pyrazol-4-yl)propane-1,3-dione (HL) and 1,10-phenanthroline (Phen) in the presence of a base afforded complex $[Nd(L)_3Phen]$ (**I**). Unstable solvate $\mathbf{I} \cdot 2CH_2Cl_2$ was obtained from a solution of the complex in dichloromethane, and its structure was determined by X-ray diffraction analysis. The photophysical properties of the complex were studied. Possible routes for the energy transfer in the course of photoluminescence were proposed.

DOI: 10.1134/S1070328414010060

INTRODUCTION

Complexes of some lanthanides, first of all, Nd, Er, and Yb, have attracted increased researchers' interest in recent years due to their capability of luminescing in the near-IR region (800–1600 nm) [1]. This range is of considerable interest for the development of biological markers since partially overlaps with the transparency window of biological tissues (760–1000 nm) [2], whereas the longer-wavelength radiation (1550 nm) is widely used in systems of optical fiber communication.

The luminescence of rare-earth element ions is characterized by a set of narrow emission lines, whose small width is caused by the physical nature of radiation generation due to the $f^* \rightarrow f$ transitions, which allows one to produce on their basis sources of almost monochromatic radiation.

At the same time, since transitions between like atomic orbitals are forbidden (the Laporte rule), the absorbability of the $f^* \rightarrow f$ transitions is low, due to which Ln^{3+} ions have low molar absorption coefficients ($\varepsilon \leq 10$ mol^{-1} L cm^{-1}) in inorganic matrices and solutions of salts.

A basic difference between complexes of rare-earth elements with organic ligands and inorganic analogs is a system of vibrational singlet and triplet levels of the ground and excited states in the organic ligand providing the absorption of the UV and visible radiation. Under certain conditions, the energy can be transferred from the excited triplet level of the ligand to the rare-earth element ion, due to which the sensitized luminescence of the central ion (antenna effect) is observed [3].

The efficiency of the energy transfer depends on several factors, in particular, on the difference in energies between the triplet level of the ligand and the resonance level of the rare-earth element ion. The main problem appeared when searching for efficient sensitizers for the Nd^{3+} ion is a very low energy of the resonance level $^4F_{3/2}$ (11698 cm^{-1}, 1.45 eV), whereas this value is higher for the most part of organic ligands. Nevertheless, a fairly efficient sensitization of this ion can often be attained by the rational selection of ligands.

In this work, the synthesis of the neodymium complex with 1,3-diketone of the pyrazole series, 1,3-bis(1,3-dimethyl-1*H*-pyrazol-4-yl)propane-1,3-dione (HL) and 1,10-phenanthroline (Phen) is described and its spectral and luminescence properties are studied.

EXPERIMENTAL

Ligand HL was synthesized according to a known procedure [4]. Neodymium oxide (99.9%) and solvents ("for synthesis" grade) were purchased from Aldrich (USA) and used as received.

Absorption spectra of solutions were recorded on a PerkinElmer Lambda 55 spectrophotometer in cells with an absorbing layer thickness of 1 cm. Luminescence spectra were detected on a Horiba Jobin-Yvon Fluorolog 3 instrument using a pulse xenon lamp for excitation and on a Maya PRO instrument using semiconductor lasers radiating at the wavelengths 365 and 805 nm and having the same radiation power (10 mW).

Synthesis of $[Nd(L)_3Phen]$ (I). Neodymium oxide Nd_2O_3 (2.102 g) was dissolved in a minimum amount of concentrated HCl (special purity grade), and the solution was evaporated to a minimum volume in a water bath and transferred to a 25-mL volumetric

flask. The volume was brought to the mark with distilled water to obtain a 0.5 M solution of $NdCl_3$.

Ligand HL (0.781 g, 3 mmol) and Phen (0.180 g, 1 mmol) were dissolved in ethanol (15 mL), and 1 M NaOH (3 mL) and a solution of $NdCl_3$ (2 mL) were consequently added dropwise with stirring. The greenish-blue solution that formed was filtered, stored at 60°C for 1 h, and left to stand at 24 h at room temperature. Then the solvent was evaporated to dryness, and the residue was extracted on heating with 30 mL of a mixture of anhydrous ethanol with CH_2Cl_2 (1 : 5 vol/vol). The solution was filtered and left in an open beaker at room temperature. After 24 h, precipitated crystals were separated, washed with MeCN, and dried in air at 45°C to a constant weight. The yield of the blue-green finely crystalline powder was 0.36 g (33%).

For $C_{51}H_{53}N_{14}O_6Nd$

anal. calcd., %: C, 55.57; H, 4.85; N, 17.79; Nd, 17.79.

Found, %: C, 55.73; H, 4.99; N, 17.81; Nd, 17.61.

X-ray diffraction analysis. Blue-green crystals of $\mathbf{I} \cdot 2CH_2Cl_2$ (**Ia**) suitable for X-ray diffraction analysis were obtained by the slow evaporation of a saturated solution of complex **I** in dichloromethane. Reflection intensities were measured on a Bruker APEX II CCD diffractometer (ω scan mode, $2\theta < 58°$). The structure was solved by a direct method and refined by the full-matrix least-squares method for F^2 in the anisotropic–isotropic approximations. All calculations were performed using the SHELXTL PLUS 5 program package [5, 6].

An analysis of the difference Fourier syntheses showed that the solvate molecules of dichloromethane were disordered over several positions. Since we failed to describe correctly the character of disordering by the refinement, the contribution of the solvate molecules to the structural scattering amplitudes was excluded using the SQUEEZ program [7, 8]. The positions of the H(C) hydrogen atoms were calculated geometrically. All hydrogen atoms were refined in the isotropic approximation by the riding model. The final value of *R* factor for **Ia** was $wR_2 = 0.0864$ for all independent reflections. The crystallographic data and refinement parameters for compound **Ia** are given in Table 1. Selected bond angles and bond lengths for compound **Ia** are listed in Table 2.

The coordinates of atoms, bond lengths and bond angles, and temperature parameters were deposited with the Cambridge Crystallographic Data Centre (no. 937136, deposit@ccdc.cam.ac.uk or http://www.ccdc.cam.ac.uk).

Table 1. Crystallographic data and experimental parameters for complex **Ia**

Parameter	Value
Empirical formula	$C_{53}H_{57}N_{14}O_6Cl_4Nd$
Temperature, K	100(2)
Wavelength (MoK_α)	0.71073 Å
Crystal system	Monoclinic
Space group	$P2_1/n$
a, Å	11.950(5)
b, Å	19.882(4)
c, Å	24.884(8)
β, deg	91.343(8)
V, Å^3	5910.56
Z	4
ρ_{calcd}, g/cm^3	1.430
$\mu(MoK_\alpha)$, mm^{-1}	1.118
T_{min}/T_{max}	0.783/0.833
$F(000)$	2596
θ_{min}–θ_{max}, deg	1.87–29.00
Number of collected reflections	69780
Number of independent reflections (R_{int})	15715 (0.0687)
Number of reflections with $I > 2\sigma(I)$	11438
Number of refined parameters	649
$R(F)$ ($I > 2\sigma(I)$)	0.0626
wR (F^2)	0.1492
Goodness-of-fit	1.085
$\Delta\rho_{max}$, $\Delta\rho_{min}$, e Å^{-3}	2.046, –2.240

RESULTS AND DISCUSSION

Compound **Ia** was synthesized according to the following scheme:

Table 2. Selected bond lengths and bond angles in compound **Ia**

Bond	*d*, Å	Bond	*d*, Å
Nd(1)–O(1)	2.363(3)	Nd(1)–O(5)	2.384(3)
Nd(1)–O(2)	2.439(3)	Nd(1)–O(6)	2.420(3)
Nd(1)–O(3)	2.389(4)	Nd(1)–N(1)	2.662(4)
Nd(1)–O(4)	2.405(4)	Nd(1)–N(2)	2.698(4)
Angle	ω, deg	Angle	ω, deg
O(1)Nd(1)N(1)	150.3(1)	N(2)Nd(1)O(4)	74.5(1)
O(1)Nd(1)O(2)	71.7(1)	N(2)Nd(1)O(5)	76.4(1)
O(1)Nd(1)N(2)	148.6(1)	N(2)Nd(1)O(6)	72.8(1)
O(1)Nd(1)O(3)	87.2(1)	O(3)Nd(1)O(4)	70.6(1)
O(1)Nd(1)O(4)	85.9(1)	O(3)Nd(1)O(5)	147.3(1)
O(1)Nd(1)O(5)	76.3(1)	O(3)Nd(1)O(6)	142.0(1)
O(1)Nd(1)O(6)	111.8(1)	O(4)Nd(1)O(5)	80.1(1)
N(1)Nd(1)O(2)	82.0(1)	O(4)Nd(1)O(6)	140.1(1)
N(1)Nd(1)N(2)	60.8(1)	O(5)Nd(1)O(6)	70.7(1)
N(1)Nd(1)O(3)	73.5(1)	Nd(1)O(1)C(14)	138.6(3)
N(1)Nd(1)O(4)	107.8(1)	Nd(1)N(1)C(2)	121.0(4)
N(1)Nd(1)O(5)	131.1(1)	Nd(1)N(1)C(13)	119.7(3)
N(1)Nd(1)O(6)	74.7(1)	Nd(1)O(2)C(16)	134.5(3)
O(2)Nd(1)N(2)	137.3(1)	Nd(1)N(2)C(11)	122.0(3)
O(2)Nd(1)O(3)	77.5(1)	Nd(1)N(2)C(12)	118.0(3)
O(2)Nd(1)O(4)	141.7(1)	Nd(1)N(2)C(12)	118.0(3)
O(2)Nd(1)O(5)	121.8(1)	Nd(1)O(3)C(27)	138.3(3)
O(2)Nd(1)O(6)	77.98(9)	Nd(1)O(4)C(29)	137.4(3)
N(2)Nd(1)O(3)	108.2(1)	Nd(1)O(5)C(40)	135.4(3)

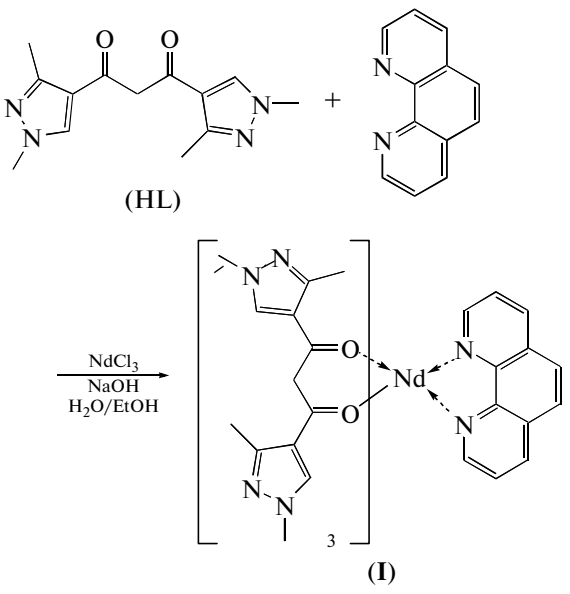

The formation of the neutral complex is complicated by the formation of basic salts, whose admixture is removed by the filtration of the solution before crystallization. Probably, a solvate is primarily formed upon the evaporation of the solution in an EtOH–CH_2Cl_2 mixture; however, the solvate is completely desolvated upon subsequent drying in vacuo.

Solvate **Ia** gradually decomposes at room temperature but is stable at 100 K, which makes it possible to study its structure by X-ray diffraction analysis. The molecular structure of compound **Ia** is shown in Fig. 1.

The coordination polyhedron of the Nd atom is a distorted tetragonal antiprism $\{NdN_2O_6\}$, whose one "cap" is formed by the O(1)–O(4) atoms and the second cap is formed by the O(5), O(6), N(1), and N(2) atoms. The average Nd–O bond lengths for both "caps" are almost equal (2.399 and 2.402 Å, respectively). The average Nd–N bond length is 2.680 Å. It should be mentioned that the average Nd–O and Nd–N bond lengths in complex **Ia** are comparable to those in complexes of a similar structure with other ligands. In particular, for complex $[Nd(tta)_3(Bipy)]$, the average Nd–O bond length is 2.453 Å and Nd–N is 2.706 Å [9].

The pyrazole fragments are somewhat unfolded relatively to the planar diketone fragment (the maximum torsion angle between the C(41)–C(40) and C(43)–C(46) bonds is 32.5°), probably, due to the general steric overloading of the molecule. Some bent of the whole molecule is simultaneously observed (the angle between the plane passing the C(39), C(40), C(41), O(5), and O(6) atoms and the line passing through the C(40) and C(42) atoms is 10.4°). Similar distortions of the structure have previously been described for the europium complexes [10].

Complex **I** is colored in blue-green and, hence, absorbs in the visible spectral range. However, as mentioned above, the molar absorption coefficients in the visible range are low and, therefore, solutions of complex **I** in MeCN (for 200–450 nm) and in DMSO (for 450–1100 nm) were used for recording the total spectrum in a range of 200–1100 nm. The solubility of the complex in MeCN is insufficient to obtain the spectra of an appropriate quality in the visible and near-IR ranges. The absorption spectra are presented in Figs. 2 and 3.

A combination of two ligands provides the efficient light absorption by the complex in the whole range from 200 to 370 nm, and the molar absorption coefficient ε attains values of 5×10^4 mol^{-1} L cm^{-1}.

The light absorption in the long-wavelength range is caused by theNd^{3+} ion only and consists of narrow bands related to the transitions from the ground level $^4I_{9/2}$ to higher energy levels. The molar absorption coefficients do not exceed 60 mol^{-1} L cm^{-1} for the most intense band at 583 nm.

The excitation spectrum of complex **I** in the crystalline state (λ_{em} = 1058 nm) is shown in Fig. 4. A characteristic feature of this spectrum is the presence

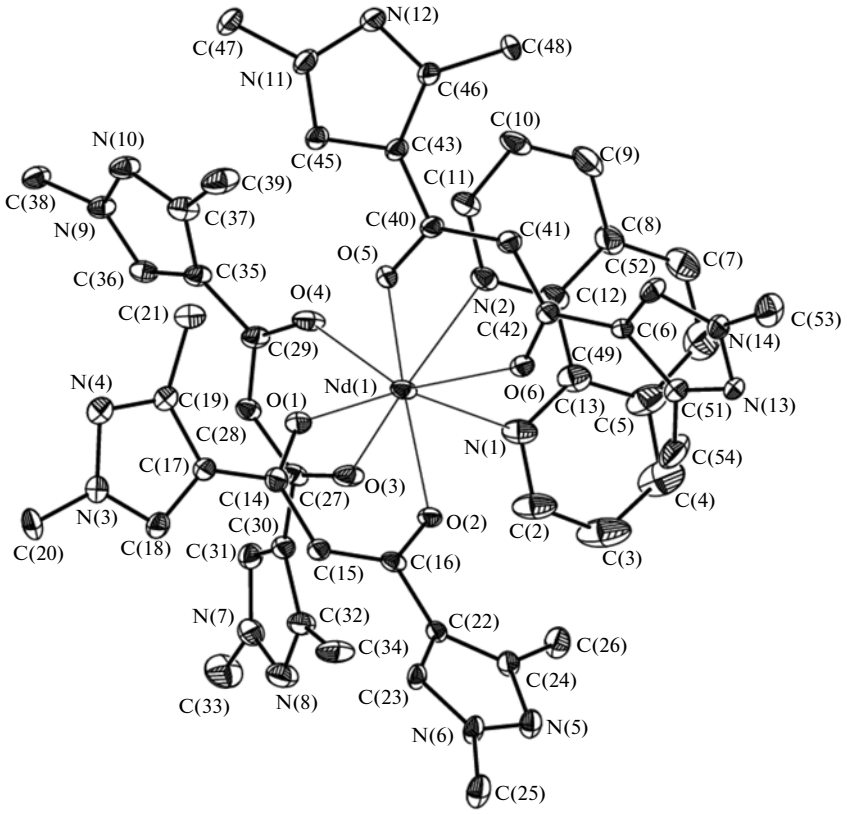

Fig. 1. Molecular structure of complex **Ia**. Thermal ellipsoids are presented with 50% probability.

of local maxima in the visible range (at 524 and 580 nm) coinciding with the corresponding lines in the absorption spectrum of the complex.

Thus, it can be assumed that the NIR luminescence of the complex can be excited by both UV and visible light if the wavelength coincides with the absorption maximum and the radiation power is sufficient.

The luminescence spectrum of complex **I** excited with a xenon lamp (λ_{exc} = 360 nm) is shown in Fig. 5. The line at 880 nm ($^4F_{3/2} \rightarrow {}^4I_{9/2}$) is strongest, and the characteristic lines at 1058 and 1340 nm ($^4F_{3/2} \rightarrow {}^4I_{13/2}$) typical of the emission spectra of the Nd^{3+} [11] are also observed.

The ratio of intensities of particular lines depends on the environment of the central ion and does not always coincide with that observed in the given case. In particular, for complex $[Nd(CF_3COO)_3(Bipy)(H_2O)_3]$ [12], the line at 1050 nm corresponding to the $^4F_{3/2} \rightarrow {}^4I_{11/2}$ transition is the strongest line upon excitation with the short-wavelength radiation.

The total energy diagram of levels of the Nd^{3+} ion is very complicated; however, only some of them, which are presented in the simplified diagram (Fig. 6), are important for the explanation of processes that occur in the course of the absorption and luminescence of complex **I**. After the absorption of the short-wavelength radiation, the energy is primarily transferred to the excited singlet levels (S_1 and higher-lying) of the organic moiety of the complex, and then different routes of the "unloading" of these levels occur.

In particular, the energy can be transferred to the low-energy triplet levels of the ligand. Since the transition with the spin change ($T_1 \rightarrow S_0$) is forbidden by the selection rules (although this forbiddance is partially eliminated in the case of lanthanide complexes due to the spin-orbital interaction), the nonradiative energy loss is observed or the transition occurs to close in energy levels of the Nd^{3+} ion.

The Nd^{3+} ion has many energy levels [13], including those close in energy to the triplet levels of the used ligands (for example, $^4G_{9/2}$, $^4G_{5/2}$, $^2G_{7/2}$, and others) to which the energy can be transferred. However, the fluorescence can be emitted not from any but only from the so-called resonance levels (in this case, $^4F_{3/2}$).

The value of triplet level T_1 for HL has been determined earlier (20023 cm^{-1}, 2.48 eV) [14], and that for Phen is 22075 cm^{-1} (2.74 eV) [15]. Thus, the energy "gap" between the triplet and resonance levels is too large (8325 cm^{-1}, 1.03 eV and 10377 cm^{-1}, 1.28 eV, respectively), which excludes the direct energy transfer. Nevertheless, a cascade mechanism of energy transfer through a series of intermediate levels is possible. Evidently, nonradiative energy losses are possible

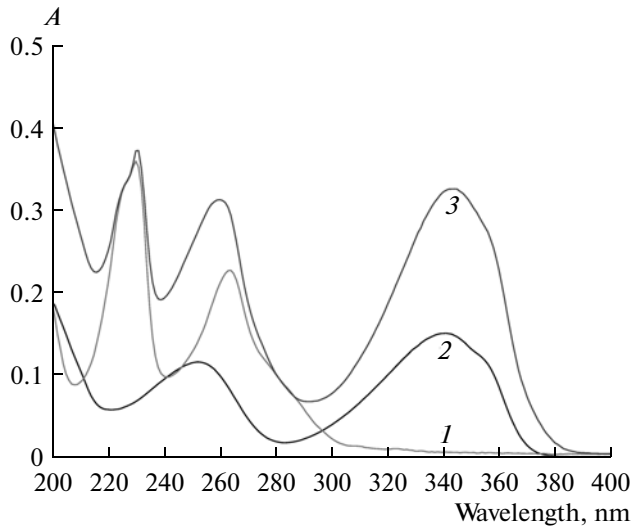

Fig. 2. Absorption spectra of (*1*) 1,10-phenanthroline, (*2*) free ligand, and (*3*) complex **I** in acetonitrile in the range from 200 to 400 nm; $c_{Phen} = 3 \times 10^{-5}$, $c_L = 3 \times 10^{-5}$, and $c_{complex} = 7.5 \times 10^{-6}$ mol/L.

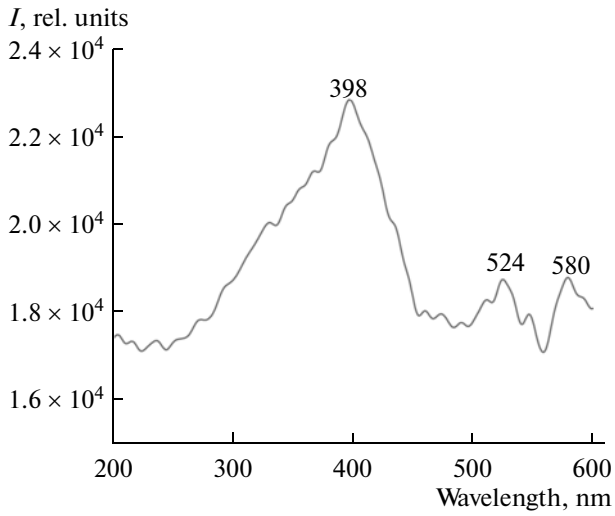

Fig. 4. Excitation spectrum of complex **I** ($\lambda_{em} = 1058$ nm).

at each step of the cascade, so that the total efficiency of sensitization is very low.

A quite different excitation process takes place if the wavelength of the exciting radiation exactly coincides with one of absorption maxima of the Nd^{3+} ion itself. For this purpose, we used a laser with a wavelength of 805 nm coinciding with one of the maxima of the absorption spectrum (transition $^4I_{9/2} \rightarrow {}^4F_{5/2} + {}^4H_{9/2}$). In this case, the central ion can selectively be excited, and the back energy transfer to the organic moiety of the complex is impossible because of a high difference in energies of the $^4F_{5/2}$ level and triplet levels of the ligands. As a result, the characteristic emission from the resonance $^4F_{3/2}$ level can be observed. In this case, complex **I** behaves similarly to inert matrices such as glasses or inorganic crystals dopped with neodymium ions [16].

The fine structure of the spectrum also changes, although the wavelength of the main line again corresponds to the $^4F_{3/2} \rightarrow {}^4I_{9/2}$ transition. To understand this phenomenon, one should keep in mind that in the real Nd^{3+} ion each level is not discrete in energy but represents a set of closely lying sublevels. For comparison, the luminescence spectra of complex **I** obtained under similar conditions using two lasers of the same

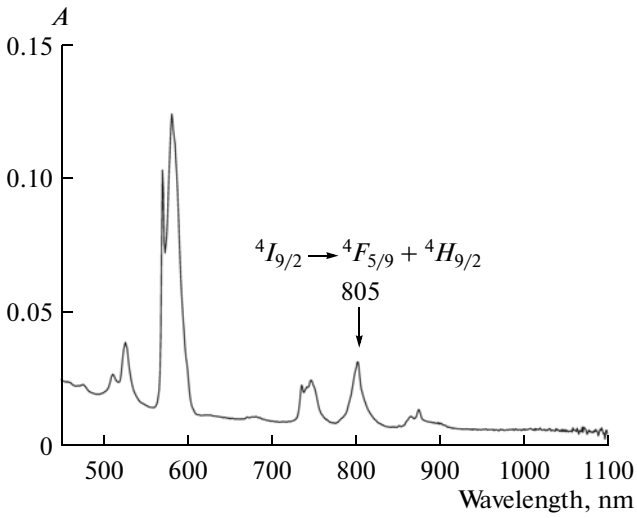

Fig. 3. Absorption spectrum of a 2.1×10^{-3} M solution of complex **I** in DMSO in the range from 450 to 1100 nm.

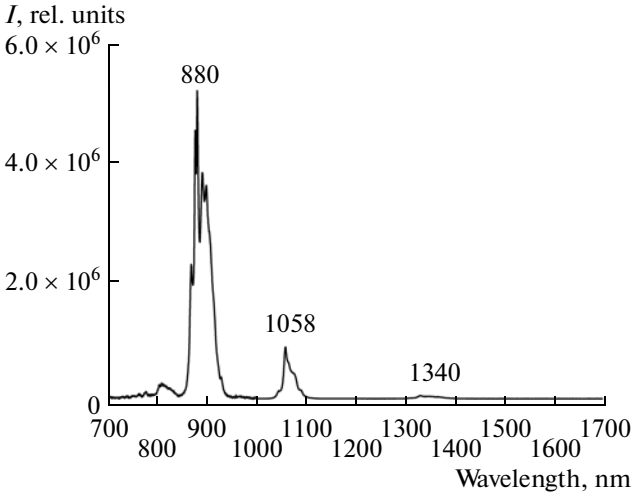

Fig. 5. Emission spectrum of complex **I** upon excitation with a xenon lamp ($\lambda_{exc} = 360$ nm).

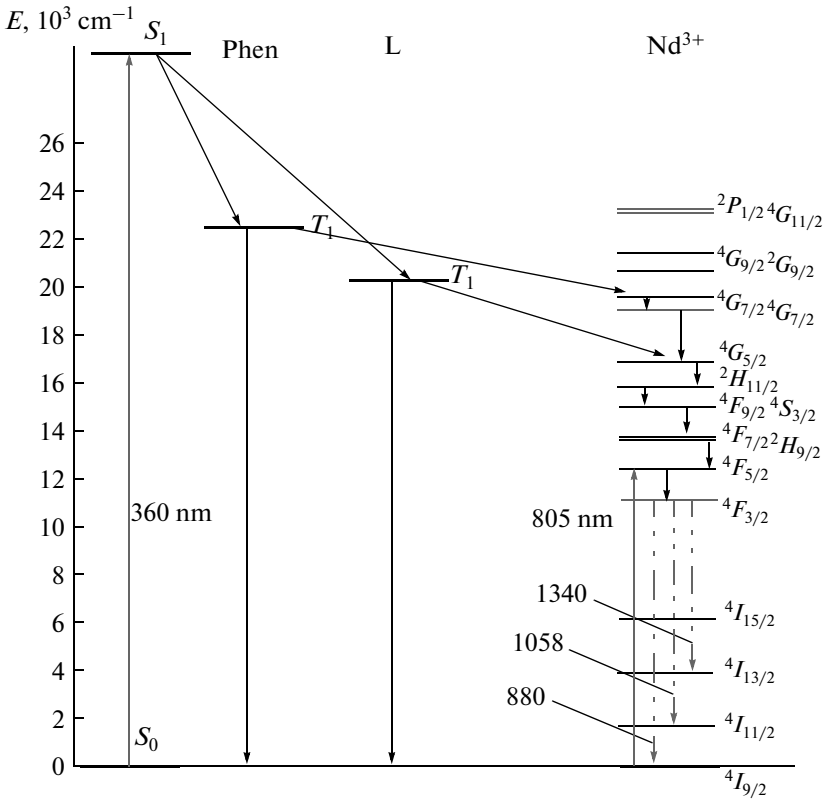

Fig. 6. Possible routes for the energy transfer in complex **I**.

power (10 mW, at 360 and 805 nm) are presented for comparison in Fig. 7.

It should be mentioned that the luminescence intensity is almost equal in both cases, i.e., the direct excitation of the Nd^{3+} ion is very efficient. Since semiconductor lasers with the necessary radiation wavelength, monochromaticity, and power are available, their use makes it possible to propose an alternative approach to the excitation of neodymium-based fluorescent labels, excluding the necessity to search for highly efficient sensitizing ligands.

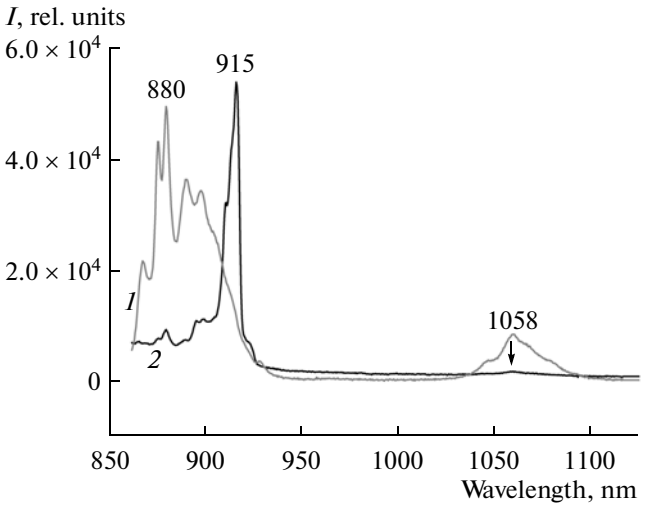

Fig. 7. Emission spectrum of complex **I** upon laser excitation with the wavelengths (*1*) 360 and (*2*) 805 nm.

ACKNOWLEDGMENTS

The authors are grateful to K.A. Lyssenko (Nesmeyanov Institute of Organoelement Compounds, Russian Academy of Sciences, Moscow) for performing X-ray diffraction analysis.

REFERENCES

1. Binnemans, K., in *Handbook of the Physics and Chemistry of Rare-Earths*, Gschneidner, K.A., Bunzli, J.G., Pecharsky, V.K., Eds., New York: Elsevier, 2005, vol. 35, p. 107.
2. Zimnyakov, D.A. and Tuchin, V.V., *Kvant. Elektronika*, 2002, vol. 32, no. 10, p. 849.
3. Rusakova, N.V., Meshkova, S.B., Venchikov, V.Ya., et al., *Zh. Prikl. Spektrosk.*, 1992, vol. 56, nos. 5–6, p. 799.
4. Taydakov, I.V. and Krasnosel'skii, S.S., *Khim. Geterotsikl. Soedin.*, 2011, no. 6, p. 843.
5. *APEX II (version 2.0-1), SADABS (version 2004/1)*, Madison (WI, USA): Bruker AXS Inc., 2005.

6. Sheldrick G.M., *SHELXTL PLUS (version 5.10). Structure Determination Software Suite*, Madison (WI, USA): Bruker AXS Inc. 1998.
7. Spek, A.L., *PLATON: A Multipurpose Crystallographic Tool*, Utrecht (The Netherlands): Utrecht Univ., 1999.
8. Sheldrick, G.M., *Acta Crystallogr., Sect. A: Found. Crystallogr.*, 2008, vol. 64, p. 112.
9. Leipoldt, J.G., Bok, D.C.L., Basson, S.S., et al., *J. Inorg. Nucl. Chem.*, 1976, vol. 38, p. 1477.
10. Puntus, L.N., Lyssenko, K.A., Bunzli, J.-C.G., et al., *J. Phys. Chem., B*, 2009, vol. 113, p. 9265.
11. Chen, D., Wang, Y., Yu, Y., et al., *Mater. Sci. Eng., B*, 2005, vol. 123, p. 1.
12. She, J., Li, D., Hou, C., et al., *J. Rare. Earths*, 2011, vol. 29, p. 193.
13. Wyart, J.-F., Meftah, A., Bachelier, A., et al., *J. Phys. B*, 2006, vol. 39, p. L77.
14. Taydakov, I.V., Zaitsev, B.E., Krasnosel'skii, S.S., et al., *Russ. J. Inorg. Chem.*, 2011, vol. 56, no 3, p. 345.
15. Xu, C., *Monatsh. Chem.*, 2010, vol. 141, p. 631.
16. Binnemans, K., Van Deun, R., Gorller-Walrand, C., et al., *J. Alloys Comp.*, 1998, vols. 275–277, p. 455.

Translated by E. Yablonskaya